Anomalous temperature dependence of photoluminescence spectra from InAs/GaAs quantum dots grown by formation–dissolution–regrowth method*

Guan-Qing Yang(杨冠卿)[1,2], Shi-Zhu Zhang(张世著)[1,2], Bo Xu(徐波)[1,2,†], Yong-Hai Chen(陈涌海)[1,2], and Zhan-Guo Wang(王占国)[1,2]

[1] *Key Laboratory of Semiconductor Materials Science, Institute of Semiconductors, Chinese Academy of Sciences, Beijing* 100083, *China*
[2] *University of Chinese Academy of Sciences, Beijing* 100049, *China*

(Received 17 January 2017; revised manuscript received 27 March 2017; published online 20 April 2017)

Two kinds of InAs/GaAs quantum dot (QD) structures are grown by molecular beam epitaxy in formation–dissolution–regrowth method with different *in-situ* annealing and regrowth processes. The densities and sizes of quantum dots are different for the two samples. The variation tendencies of PL peak energy, integrated intensity, and full width at half maximum versus temperature for the two samples are analyzed, respectively. We find the anomalous temperature dependence of the InAs/GaAs quantum dots and compare it with other previous reports. We propose a new energy band model to explain the phenomenon. We obtain the activation energy of the carrier through the linear fitting of the Arrhenius curve in a high temperature range. It is found that the GaAs barrier layer is the major quenching channel if there is no defect in the material. Otherwise, the defects become the major quenching channel when some defects exist around the QDs.

Keywords: quantum dot, photoluminescence, anomalous temperature dependence, activation energy

PACS: 81.07.Ta, 78.55.–m, 82.20.Pm **DOI:** 10.1088/1674-1056/26/6/068103

1. Introduction

Semiconductor quantum dot (QD) lasers have attracted considerable attention as the most promising light sources for future communication, owing to their low threshold current densities, high temperature stabilities,[1–3] longer wavelengths, high modulation speeds, and low chirps.[4–7] The performances of the QD lasers are directly related to the optical properties of the QD materials.[8] Photoluminescence (PL) spectroscopy is an effective technique to characterize the optical properties of the QD materials. In particular, by analyzing the PL spectrum variations with temperature, we can deduce the quenching channel of QD material.[9–11] Thermionic emission of the photo-excited carriers out of the QD potential was found to be a dominant mechanism leading to the thermal quenching of the PL in self-assembled quantum dots (QDs).[9,10,12,13] Xu *et al.*[11,14] grew a number of self-organized InAs/GaAs heterostructures with InAs layer thickness values from 0.5 ML to 3 ML, then investigated the temperature dependence of PL properties of the samples. They found that for InAs mono-layers or sub-mono-layers the barrier for the thermionic emission of carriers is GaAs, while for high-quality InAs multi-layers the wetting layer might serve as a barrier. Dai *et al.*[15] found that the emission intensity quenched rapidly when the temperature rose to around 60 K, indicating the existence of defect-related center in the vicinity of InAs/GaAs interface. They suggested that the PL quenching was dominated by defect-related centers instead of GaAs in their case. Huang *et al.*[16] grew extremely low density InAs QDs by molecular beam droplet epitaxy. They deposited a proper amount of gallium (Ga) to saturate the excess As atoms that were present on the substrate surface. Then In atoms were deposited on the GaAs buffer layer, forming InAs QDs. No wetting layer connecting the QDs was observed, and no typical temperature-related PL properties of QDs formed by the Stranski–Krastanov (S-K) growth mode were shown either. The peak energy did not show super-fast redshift and the full width at half maximum (FWHM) did not transform with the temperature increasing either. It meant that wetting layer was the transfer channel of carriers in regular S-K QDs.

In this paper, we report a formation–dissolution–regrowth[17] (FDR) method to fabricate low-density, longer-wavelength InAs/GaAs QDs, for the future application in single-photon light sources in fiber-based quantum communication.[18–26] The temperature dependence of PL peak energy, intensity, and FWHM of the samples were studied. We found that it was different from the results reported previously.[9,10]

2. Material growth and characterizations

Two kinds of samples were grown on GaAs (100) substrates in a Veeco Mod GenII solid-source molecular beam epitaxy (MBE) system. A 100-nm GaAs buffer layer, a

*Project supported by the National Basic Research Program of China (Grant No. 2013CB632104) and the National Key Research and Development Program of China (Grant No. 2016YFB0402302).

†Corresponding author. E-mail: srex@semi.ac.cn

© 2017 Chinese Physical Society and IOP Publishing Ltd

GaAs/AlGaAs superlattice, and another 100-nm GaAs layer were grown consecutively at 580 °C as shown in Fig. 1. Afterwards, a layer of buried QDs was grown for PL study. We grew 1.5 mono-layer (ML) InAs QD layer at 490 °C with a growth rate of 0.01 ML/s, and then annealed both samples for 1 min. The growth of QDs was ended for sample A, but sample B was then heated up to 530 °C in 168 s and kept at this temperature for 30 s, then a 0.2-ML InAs layer was deposited in 20 s, and the sample was cooled to 490 °C in 168 s.

Thereafter, a 15-nm GaAs cap layer was grown on the InAs QD layer at 490 °C, and a 285-nm GaAs was grown at 580 °C for both samples.

Finally, we grew a surface InAs quantum dot layer on the top of GaAs for each sample in the same way as for the buried quantum dot layer, in order to observe the quantum dot morphology.

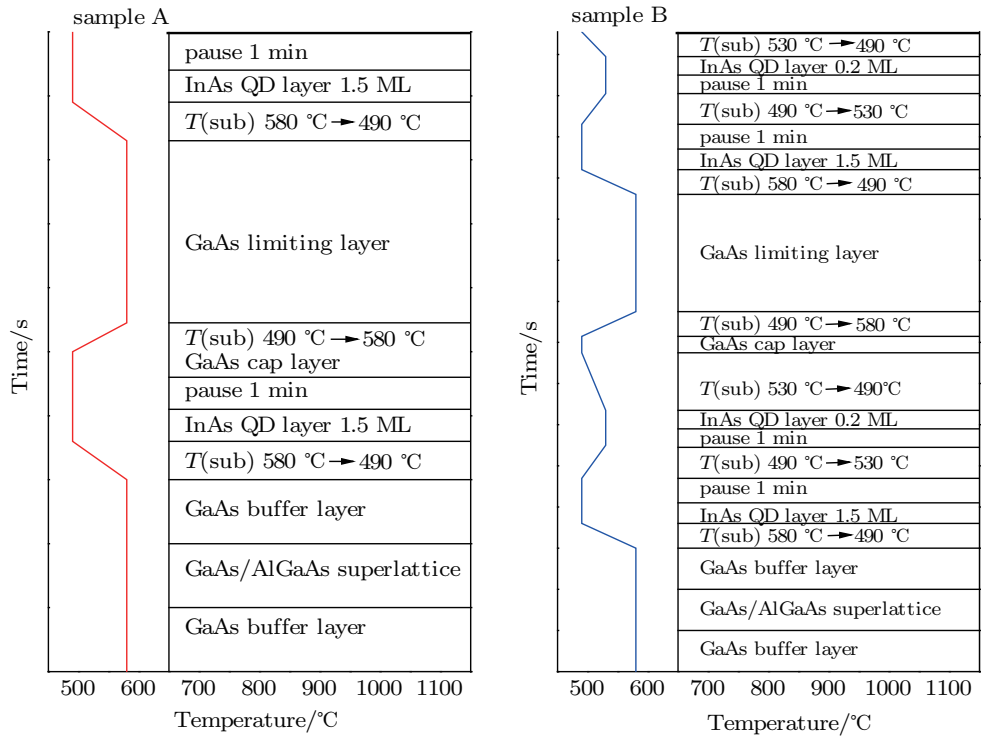


Fig. 1. (color online) Growth times versus temperature and the layer structures of samples A and B.

The surface morphology was imaged by a Solver P47 atomic force microscope (AFM) system. Photoluminescence (PL) measurements were performed using a Fourier transform infrared spectrometer equipped with an InGaAs detector. Both samples were excited by a 532-nm solid-state laser and mounted in a cryostat providing temperatures from 15 K to 300 K.

3. Results and discussion

In Fig. 2, the QD densities of samples A and B are 3.03×10^{10} cm^{-2} and 1.3×10^{9} cm^{-2} by AFM, respectively. We can see dual-mode size distributions in samples A and B. The average base diameters of QDs in samples A and B are 29 nm and 60 nm, respectively. The movement of In becomes rapid and small InAs QDs decompose into In atoms[27,28] because of high substrate temperature during the second stage of InAs deposition in sample B. The In atoms are easily captured by large InAs QDs which leads to the lower QD density in sample B and bigger average base diameter. At the same time, Ga atoms are easy to exchange with In atoms in InAs.[29] The strain in the wetting layer of sample B decreases and thus it is hard to form new QDs.

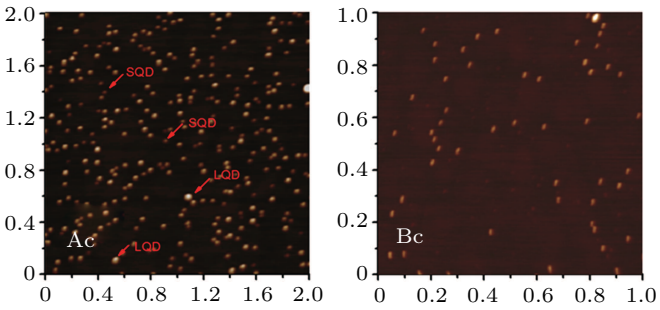


Fig. 2. (color online) AFM images for samples A (Ac) and B (Bc).

Owing to the larger QD size in sample B, the PL wavelength of sample B is considerably longer than that of sample A, reaching the 1.3 μm (0.95 eV) window of fiber communication as indicated in Fig. 3.

The temperature dependence of PL peak energy, intensity, and FWHM for samples A and B are measured and summarized in Figs. 3–7.

We analyze the relationship between experiment value of PL peak energy and theoretical Varshni value. The equation of Varshni[30] describes the theoretical PL peak energy versus

temperature, which is

$$E_g(T) = E_g(0) - \frac{\alpha T^2}{T+\beta},$$

where $\alpha = 2.76 \times 10^{-4}$ eV/K and $\beta = 93$ K; $E_g(T)$ and $E_g(0)$ denote the band gaps when temperatures are equal to T and 0, respectively; the black curves in Fig. 3 represent the Varshni value versus temperature. In Fig. 3(a), PL peak energy is red-shifted by 119 meV with temperature rising from 15 K to 300 K, while Varshni curve is red-shifted by only 62.7 meV. It indicates that QDs are variable in size in sample A. In Fig. 3(b), PL peak energy is red-shifted by 74.2 meV with temperature rising from 14 K to 300 K, compared with 62.7 meV of Varshni curve. It suggests that QDs are nearly uniform in size for sample B.

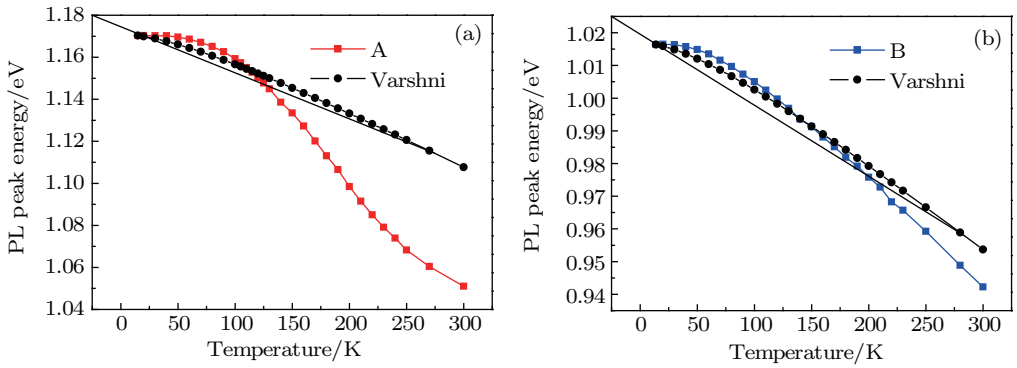


Fig. 3. (color online) Plots of PL peak energy and Varshni value versus temperature for samples A and B.

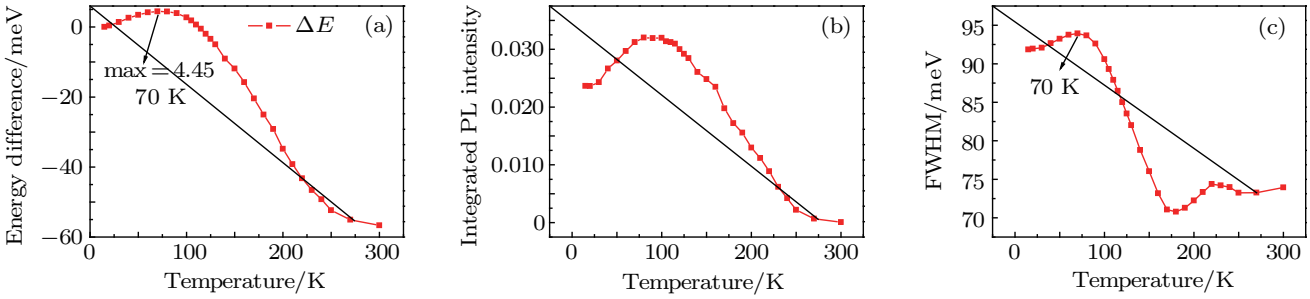


Fig. 4. (color online) Temperature dependence of energy difference between experimental value and Varshni value (a), integrated PL intensity (b), FWHM of PL spectra (c) for sample A.

Focusing on the low temperature part ($T < 70$ K) of the curves in Figs. 4(a) and 4(c), we can find that the experimental peak energy of sample A is higher than Varshni value, which means a "slow redshift", in contrast to the "super-fast redshift" generally reported in PL of S-K QDs. The FWHM becomes higher with temperature increasing, also different from previous reports.[9,10] At higher temperatures, we can see that the experimental PL peak redshifts much quicker than the Varshni value predicted and the peak energy goes far below the Vashni value. The FWHM decreases quickly. This seems like a typical "super-fast redshift" generally reported in normal S-K QDs. As temperatures approach 300 K, the redshift slows down, and FWHM turns up again. This is also nearly the same as the normal QDs.

To explain the phenomena in the low temperature part of the curves, we propose an energy band model as illustrated in Fig. 5.

QDs in sample A are prepared by 1.5-ML low-temperature InAs deposition followed by a growth-interruption or in situ annealing at 490 °C, and reveal the dual-mode size distribution as shown in Fig. 2. The larger quantum dots (LQDs) easily capture In adatoms and enlarge its size.[27] But it is harder for the smaller quantum dots (SQDs) to capture In adatoms. They can acquire In atoms only from the wetting layer, which leads to the thinning of the wetting layer around SQDs.[31] The wetting layer around SQDs is named WL2, while regular wetting layer is called WL1. The energy level of WL2 is higher than that of WL1 because of its smaller thickness. So WL2 acts as a shallow local potential barrier which can prevent the carriers from transferring from WL1 into SQDs at low temperature. At high temperature, the carriers in SQDs can be thermally activated through WL2 into WL1 and LQDs. If all the carriers arrive at LQDs and cause radiative recombination, the peak energy of PL is red-shifted quickly and FWHM decreases, but luminescence intensity does not quench. On the contrary, if the carriers in SQDs go to GaAs or defect energy levels, luminescence intensity quenches. The carriers in LQDs can also be activated and transferred to GaAs or defect energy levels, which leads to the quenching of luminescence intensity too.

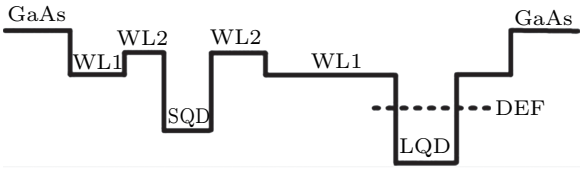


Fig. 5. Relative conduction bands of SQD, LQD, WL1, WL2, GaAs, and DEF

With the above model, the temperature dependence of PL from sample A, especially the low temperature part, can be explained as follows.

When $T < 70$ K, PL intensity and FWHM increase, but PL peak energy is red-shifted slowly. At low temperatures, the carriers in WL1 can only transfer to LQDs and recombine radiatively. With temperature increasing, the carriers in WL1 can obtain more energy to overcome the barrier between WL2 and WL1, and arrive at SQDs, in addition to the arrival at LQDs. More SQDs contribute to luminescence, in this way the PL intensity increases. The energy level of SQDs is higher than that of LQDs, thereby leading to a blueshift tendency of PL peak. However, the redshift caused by lattice expansion with increasing temperature predominates, so the PL peak energy is red-shifted finally, but more slowly than Varshni value, so that the energy difference is positive in the left part of Fig. 4(a). Because of the size difference between LQDs and SQDs, the FWHM also increases. So the anomalous PL phenomenon in S-K QDs can be observed.

When 70 K$< T <$ 110 K, PL intensity remains nearly unchanged, FWHM begins to reduce quickly, and peak energy is red-shifted quickly. At this temperature, the carriers in SQDs can obtain enough energy by thermal excitation to overcome the barrier between WL2 and SQD, and reach LQDs through carriers transfer channel WL1, finally recombining at LQDs radiatively. With less component from SQDs and more component from LQDs, the PL peak energy is red-shifted more quickly than Varshni value, and FWHM reduces. This is in accordance with the reported "super-fast redshift" in normal S-K QDs. When 110 K$< T <$ 170 K, PL intensity also decreases. Some carriers in SQDs can be thermally motivated into a quenching channel at this temperature, and recombine outside QDs, resulting in the quenching of QD PL intensity. The energy difference between QD level and quenching channel can be estimated from the activation energy (E_{A}), deduced from the linear fitting of the Arrhenius plots of temperature-dependent PL intensity at high temperatures.

From the Arrhenius equation

$$I_{\mathrm{PL}}(T) = I_0 * \exp(E_{\mathrm{A}}/kT),$$

where I_0 is the PL intensity at low temperature, $I_{\mathrm{PL}}(T)$ is the PL intensity at temperature T, and E_{A} is the activation energy of the carriers thermally running away. In Fig. 6, at high temperatures, the curves each tend towards a straight line due to an exponential quenching characteristic, and E_{A} can be deduced by measuring the slope. The E_{A} of sample A is determined to be 376 meV, just the difference between the QD level (1.051 eV) and GaAs band gap (1.42 eV) at 300 K. So we can confirm that the quenching channel in sample A is GaAs barrier layer.

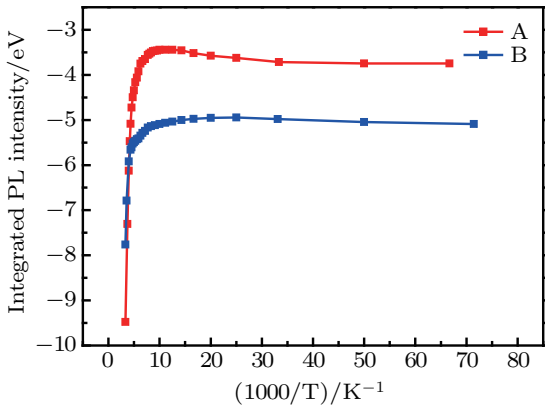


Fig. 6. (color online) Arrhenius plots of the temperature dependence of the integrated PL intensity for samples A and B

When 170 K$< T <$ 220 K, PL intensity decreases, peak energy keeps redshifting and FWHM increases. Carriers in SQDs continue transferring into LQDs and GaAs barrier layer, the former causes the continued redshift of peak energy and the latter causes the continued quenching of PL intensity. With the increase of temperature, electron–phonon scattering becomes more and more active, therefore the FWHM increases. When 220 K$< T <$ 300 K, PL intensity keeps decreasing, peak energy redshift slows down, and FWHM first decreases and then increases. At this temperature, most carriers are distributed in LQDs rather than SQDs, some even occupy the excited states of LQDs. So the red-shifting tendency is partly compensated for and slowed down. Some carriers continue to be thermally motivated into GaAs barrier layer, causing the PL intensity to quench. The FWHM is determined by the competition between the decreasing tendency caused by the residual carriers transferring from SQDs to LQDs and the increasing tendency caused by stronger electron–phonon scattering and carrier occupation in excited LQD levels. The increasing tendency will be dominant finally.

To conclude, the existence of the WL2 barrier in sample A causes more carriers to be able to arrive at SQDs at increased temperatures in the $T < 70$ K range, resulting in the anomalous behavior of the PL spectrum. With further increasing temperatures, the carriers in SQDs can arrive at LQDs or GaAs through WL2 and WL1, causing the peak energy to be super-quickly red-shifted and the PL intensity to quench, and the FWHM to narrow.

For sample B, the experimental peak energy is also higher than the Varshni value, and FWHMs go higher with increasing temperatures in the low temperature region of the curves as shown in Figs. 7(a) and 7(c), also different from the generally reported "super-fast redshift" in PL of S-K QDs in the literature. At higher temperatures, the experimental PL peak is red-shifted a little bit more quickly than Varshni value predicted, and the peak energy goes below the Vashni value to a small extent. The FWHM begins to decrease slowly at higher temperatures.

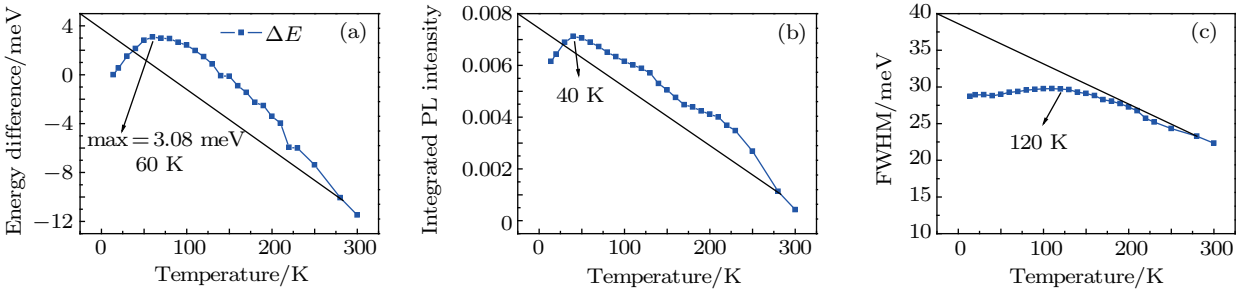


Fig. 7. (color online) Temperature-dependent energy difference between experimental value and Varshni value (a), integrated PL intensity (b), FWHM of PL spectra (c) for sample B.

These phenomena can also be explained by the above energy band model, with the supplementation of a defect energy level (DEF).

QDs in sample B are prepared by 1.5-ML low-temperature InAs deposition followed by an interruption/in-situ annealing at a higher temperature of 530 °C, and the re-growth of 0.2-ML InAs at the same temperature. The density of dots is much lower, and their size is more uniform as illustrated in Fig. 2. The sizes of dots are also much bigger than those of sample A, resulting in a longer wavelength of 1.32 μm at 300 K. Since the QDs are very large, some defects may be formed around them during the capping with GaAs, and the long-time high-temperature interruption/annealing can also introduce some defects. The carriers in LQDs can be thermally activated into the defect energy level and recombine non-radiatively there.

The defect energy level can be located from Fig. 6. The E_A of sample B is determined to be 147 meV, which is far lower than the difference between the QD level (0.945 eV) and WL1 level ($\sim$ 1.38 eV) at 300 K. This indicates that the quenching channel/defect level is located between the LQD and WL1.

When $T < 40$ K, PL intensity increases, FWHM increases a little, and PL peak energy is red-shifted slowly. The reason is the same as in the $T < 70$ K range in sample A, except that the size of QDs in sample B is more uniform, so that the FWHM only increases a little.

When 40 K$< T <$ 60 K, PL intensity begins to decrease, FWHM keeps on increasing slowly, and PL peak energy keeps redshifting slowly. Carriers in WL1 continue to overcome the WL2 barrier and arrive at SQDs, causing the PL peak redshifting slowly and broadening slowly. The decreasing of PL intensity also originates from thermal excitation of carriers into a quenching channel, but this time the channel is DEF around LQDs, rather than GaAs barrier layer adjacent to SQDs.

When the quenched carriers are more than the carriers injected into the SQDs, PL intensity will decrease. The quenching of LQD emission may cause the FWHM to tend to decrease, but the effect of filling of the SQDs will be dominant, so the FWHM increases gradually.

When 60 K$< T <$ 120 K, PL intensity continues to decrease, FWHM goes on increasing slowly, but PL peak energy begins to be red-shifted more quickly than Varshni predicted. In this region, the injection of carriers into SQDs through WL2 is nearly saturated, but the excited transferring of carriers from SQDs to LQDs through WL2 and WL1 has not been started, since the SQD to WL2 barrier is higher due to the longer emission wavelength of the QDs. Some carriers in SQDs may be thermally excited into the DEF quenching channel. Less emission from SQDs will lead to a redshift of the peak energy, and the PL intensity to decrease, in addition to the effect by excitation from LQDs to DEF. The FWHM may also decrease in this process, but the electron–phonon scattering will overcompensate for that effect and result in the slow increasing of FWHM.

When $T >$ 120 K, PL intensity continues to decrease, FWHM begins to decrease, and PL peak energy keeps on redshifting at a relatively quick speed. At this stage, the carriers transfer from SQDs to LQDs through WL2 and WL1 starts, resulting in the redshift of peak energy and the reduction of FWHM. Since the QDs are more uniform, the shift and reduction are relatively slow. Meanwhile the excitation of carriers from LQDs and SQDs into DEF continues, leading to further quenching of PL intensity.

In short, the existence of WL2 barrier in sample B causes more carriers to be able to arrive at SQDs with temperature increasing in the $T <$ 60 K range, resulting in the anomalous behavior of PL spectrum. Some DEFs exist around the large QDs fabricated by formation–dissolution–regrowth (FDR) method, which accounts for the thermal quenching of PL intensity from

$T > 40$ K. In the $T > 120$ K range, the carriers in SQDs can arrive at LQDs through WL2 and WL1, causing the peak energy to be red-shifted rapidly and the FWHM to narrow.

4. Conclusions and perspectives

In order to develop low-density, longer-wavelength InAs/GaAs QDs for the applications in single-photon light sources in fiber-based quantum communication, we study the temperature dependence of PL peak energy, intensity, and FWHM of two kinds of InAs/GaAs QD samples grown by MBE in formation–dissolution–regrowth method with different *in-situ* annealing and regrowth processes. It is found that the wetting layer around smaller QDs is thinner than elsewhere, and serves as an energy barrier for the carriers to be injected into small QDs. This gives rise to the anomalous temperature dependence of PL spectrum in a low temperature range, including slower redshift, increase in intensity and FWHM.

It is also found that some defects may be formed around the large QDs and in the long-time high-temperature interruption/annealing during growth. The defect energy level will act as a major quenching channel of PL peak intensity instead of GaAs barrier layer in this kind of sample. So the FDR growth process needs to be further optimized to reduce these defects.

References

[1] Lv X Q, Jin P and Wang Z G 2010 *Chin. Phys. B* **19** 018104
[2] Ji H M, Cao Y L, Yang T, Ma W Q, Cao Q and Chen L H 2009 *Acta Phys. Sin.* **58** 1896 (in Chinese)
[3] Wang T, Zhang J J and Liu H Y 2015 *Acta Phys. Sin.* **64** 204209 (in Chinese)
[4] Lv Z R, Ji H M, Yang X G, Luo S, Gao F, Xu F and Yang T 2016 *Chin. Phys. Lett.* **33** 124204
[5] Arakawa Y and Sakaki H 1982 *Appl. Phys. Lett.* **40** 939
[6] Bhattacharya P and Mi Z 2007 *Proc. IEEE* **95** 1723
[7] Zhukov A E, Maksimov M V and Kovsh A R 2012 *Semiconductors* **46** 1225
[8] Wang T, Liu H Y and Zhang J J 2016 *Chin. Phys. Lett.* **33** 044207
[9] Fafaxd S, Raymond S, Wang G, Leon R, Leonar D, Charbonneau S, Merz J L, Petroff P M and Bowers J E 1996 *Surf. Sci.* **361** 778
[10] Fafard S, Leon R, Leonard D, Merz J L and Petroff P M 1994 *Phys. Rev. B* **50** 8086
[11] Xu Z Y, Lu Z D, Yang X P, Yuan Z L, Zheng B Z and Xu J Z 1996 *Phys. Rev. B* **54** 11528
[12] Fafard S, Leon R, Leonard D, Merz J L and Petroff P M 1995 *Phys. Rev. B* **52** 5752
[13] Fafard S, Leonard D, Merz J L and Petroff P M 1994 *Appl. Phys. Lett.* **65** 1388
[14] Xu Z Y, Lu Z D, Yuan Z L, Yang X P, Zheng B Z and Xu J Z 1998 *Superlattices Microstruct.* **23** 381
[15] Dai Y T, Fan J C, Chen Y F, Lin R M, Lee S C and Lin H H 1997 *J. Appl. Phys.* **82** 4489
[16] Huang S S, Niu Z C, Ni H Q, Zhan F, Zhao H, Sun Z and Xia J B 2007 *Chin. Phys. B* **24** 1025
[17] Zhang S Z, Ye X L, Xu B, Liu S M, Zhou W F and Wang Z G 2013 *Chin. Phys. Lett.* **30** 087804
[18] Jiang Q Q, Li W X, Tang C C, Chang Y C, Hao T T, Pan X Y, Ye H T, Li J J and Gu C J 2016 *Chin. Phys. B* **25** 118105
[19] Zhu G, Zheng F, Wang C, Sun Z B, Zhai G J and Zhao Q 2016 *Chin. Phys. B* **25** 118505
[20] Dong Y, Wang G L, Wang H P, Ni H Q, Chen J H, Gao F Q, Qiao Z T, Yang X H and Niu Z C 2014 *Chin. Phys. B* **23** 104209
[21] Naiki H, Masuo S, MacHida S and Itaya A 2017 *J. Phys. Chem. C* **115** 23299
[22] Cheng D F, Li X, Zhang C F, Tan H, Wang C, Pang L F and Shi H C 2017 *ACS Appl. Mat. Interf.* **7** 2847
[23] Andre Schwagmann, Sokratis Kalliakos, Ian Farrer, Jonathan P Griffiths, Geb A C Jones, David A Ritchie and Andrew J Shields 2015 *Appl. Phys. Lett.* **99** 46
[24] Meyer H M, Stockill R, Steiner M, Gall C Le, Matthiesen C, Clarke E, Ludwig A, Reichel J, Atature M and Kohl M 2015 *Phys. Rev. Lett.* **114** 123001
[25] Zhang W, Shi Z W, Huo D Y, Guo X X and Peng C S 2016 *Acta Phys. Sin.* **65** 117801 (in Chinese)
[26] Shang X J, Xu J X, Ma B, Chen Z S, Wei S H, Li M F, Zha G W, Zhang L C, Yu Y, Ni H Q and Niu Z C 2016 *Chin. Phys. B* **25** 107805
[27] Heyn C, Endler D, Zhang K and Hansen W 2000 *J. Cryst. Growth* **210** 421
[28] Heyn C, Endler D, Zhang K and Hansen W 2002 *Phys. Rev. B* **66** 5237
[29] Joyce P B, Krzyzewski T J, Bell G R, Joyce B A and Jones T S 1998 *Phys. Rev. B* **58** 15981
[30] Vurgaftman I, Meyer J R and Ram-Mohan L R 2001 *J. Appl. Phys.* **89** 5815
[31] Zhou G Y, Chen Y H, Zhou X L, Xu B, Ye X L and Wang Z G 2010 *Physica E* **43** 308